Upscaling uncertainty analysis in a shallow-marine environment

Karl D. Stephen[1], Canghu Yang[1], Jonathan N. Carter[2], John A. Howell[3], Tom Manzocchi[4] and Arne Skorstad[5]

[1] *Institute of Petroleum Engineering, Heriot-Watt University, Edinburgh EH9 9NX, UK (e-mail: Karl.Stephen@pet.hw.ac.uk)*

[2] *Department of Earth Science and Engineering, Imperial College, London SW7 2BP, UK*

[3] *Department of Earth Science/Centre for Integrated Petroleum Research, University of Bergen, Allegt. N-5007, Bergen, Norway*

[4] *Fault Analysis Group, UCD School of Geological Sciences, University College Dublin, Dublin 4, Ireland*

[5] *Norwegian Computing Center, PO Box 114 Blindern, N-0314 Oslo, Norway*

ABSTRACT: Geological models are often created at a scale finer than is suitable for flow simulation and also ignore the effects of sub-cellular heterogeneities. Upscaling of static and dynamic reservoir properties is an important process that captures the impact of smaller scales, ensuring that both heterogeneity and the flow physics are represented more accurately. A Geopseudo upscaling approach for shallow-marine reservoirs is presented, which captures the essential flow characteristics across a range of scales from laminae to the simulation grid. Starting with a base-case set of minimum assumptions enables generation of one set of pseudo-relative permeability and capillary pressure curves per facies. This is then expanded to investigate the limitations of these assumptions and compare their impact against variations in large-scale geological and structural parameters. For the analysis, two-level full factorial experimental design is used to determine important parameters. A comparison of upscaling effects is also performed.

The most important upscaling and fine-scale parameters identified by the analysis are the shape of the capillary pressure curve, lamina-scale permeability variation and upscaling flow speed. Of similar importance are the sedimentological parameters for shoreline aggradation angle and curvature. Fault direction (perpendicular and parallel to the shoreline) and the fine-scale upscaling method are of moderate to low importance. The shallow-marine parameter for clinoform barrier strength and the direction of flow considered when upscaling are unimportant. Analysis of upscaling effects suggests that the algorithm used at the intermediate scale is not important, while the assumed flow speed is very important, typically resulting in a 10% maximum variation in cumulative recovery. Fine-scale properties and upscaling methods affect recovery mostly due to increased initial water saturations but also because of early breakthrough.

KEYWORDS: *Upscaling, uncertainty, shallow marine, geopseudos, sedimentary structures*

INTRODUCTION

Hydrocarbon production can be predicted using suitable geological models of reservoirs, together with accurate representation of the flow processes. In practice, geological modelling is carried out using cells measuring tens of metres horizontally and several tenths of metres vertically. To reduce simulation time, these models may be upscaled, although, usually, this is done only for static variables, such that relative permeability and capillary pressure curves from centimetre-scale measurements (special core analysis) are often used.

The common approach can lead to numerical dispersion unless small-scale heterogeneity effects spread out the flood front. Compensation for numerical dispersion can be obtained by upscaling of two-phase flow (e.g. Kyte & Berry 1975; Stone 1991), which also captures scale-dependent heterogeneity (e.g. Weber 1986; Jones *et al.* 1995) and gives pseudo-relative permeability and capillary pressure curves. Lamina-scale (millimetres to centimetres) heterogeneity can affect the shape of the saturation-dependent relative permeability and capillary pressure curves due to capillary oil trapping (Kortekaas 1985; Ringrose *et al.* 1993). The Geopseudo Method (Corbett *et al.* 1992; Corbett 1993) was developed to improve the process by upscaling in stages using representative geological models at each scale.

Upscaling of dynamic, two-phase flow properties is much more complicated than for static properties such as absolute permeability, which may be upscaled robustly when a

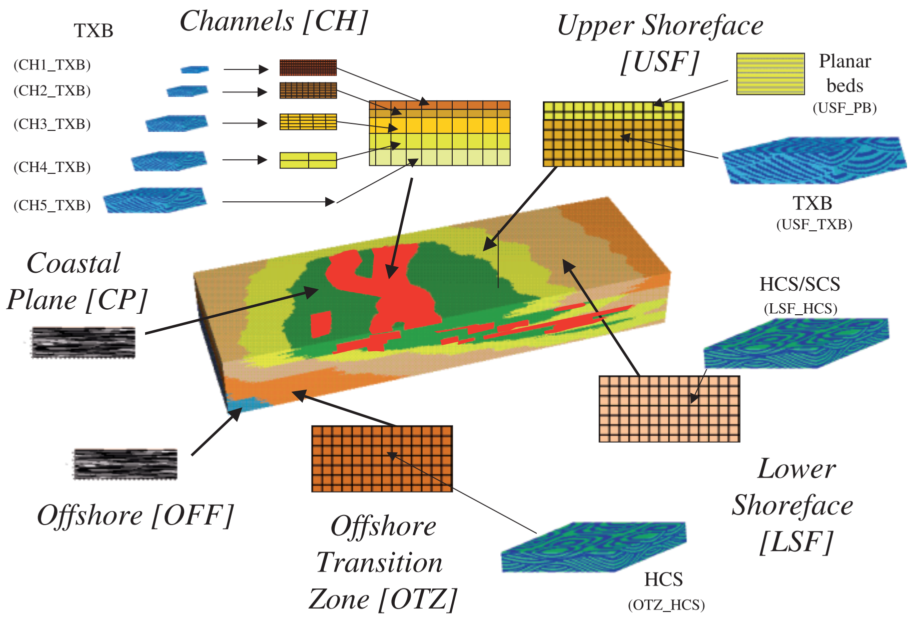

Fig. 1. Geological modelling hierarchy including six facies associations, each with internal heterogeneity. Each upscaling step is indicated by an arrow. The models of the facies at the finest scale are denoted by the terms in brackets, e.g. '(LSF_HCS)'. Details on these models can be seen in Table 1. The intermediate level models are indicated by the terms in square brackets (e.g. '[LSF]'). The size of the grid cells at this scale are $0.5 \times 0.5 \times 0.1$ m and measured $75 \times 75 \times 4$ m in total.

separation of scales occurs (Whitaker 1969). Upscaling of two-phase flow can add to the uncertainty of simulation results as the approach relies on an appropriate choice of boundary conditions, which are often assumed or approximated. Application of the Geopseudo Method (Corbett *et al.* 1992; Ringrose *et al.* 1993), however, can exploit the separation of length scales if suitable models are used. Under certain circumstances, when capillary forces dominate over viscous pressure gradients and gravity (Kortekaas 1985), capillary equilibrium may be assumed and the boundary conditions can be simplified. Ekrann *et al.* (1996) showed that this occurs for models smaller than 20 cm, and the capillary equilibrium steady state (PCE) method (Smith 1991; Pickup & Sorbie 1996) can be used. Similarly, when capillary and gravity forces are negligible, the viscous dominated steady state method may be used (Smith 1991; Kumar & Jerauld 1996). Such methods can give robust upscaling results. In other circumstances, dynamic methods of upscaling should be used, such as Kyte & Berry (K&B 1975), Stone (STO 1991), the pore volume weighted (PVW) method (Eclipse Manual 2003), the transmissibility weighted method (Darman *et al.* 1999). The suitability of the methods depends on the balance of forces (Coll & Muggeridge 2001; Stephen *et al.* 2001). Application of each method can give different results, depending on flow conditions. For a fuller discussion, see Barker & Thibeau (1997) and Christie (2001).

It is inevitable that uncertainty exists throughout the upscaling process from the acquisition and assignment of dynamic flow properties, through the construction of sedimentary and geological models at different scales, into the computational process used to obtain the pseudos. It is virtually impossible to capture the full variability of many of the parameters. The aim of this study was to determine how some of the small-scale geological and petrophysical parameters affect flow at the large scale. Also considered was the effect of different upscaling methods, although there was no intention of testing their accuracy. Such an approach would require extremely detailed models and would be computationally intensive. This is the case in most reservoirs and the choice of upscaling method is often made blindly. Instead, the aim was to quantify the effect of choosing different upscaling methods and compare these to the large-scale geological parameters, such as shoreline aggradation angle, shoreline curvature, the barrier strength of clinoforms, fault strike direction and fault permeability, which were considered as part of the SAIGUP project (Howell *et al.* 2008; Manzocchi *et al.* 2008*a*).

Using the Geopseudo approach, upscaling was carried out in two stages to represent the flow mechanisms better. The paper first presents the geological modelling and upscaling hierarchy used. Then, the derivation of a base-case set of pseudo-relative permeability and capillary pressure curves is given. These were obtained with a minimum set of assumptions to reduce complexity and provide a set of pseudos for the SAIGUP project as a whole (Matthews *et al.* 2008). Finally, an analysis is shown of how the different assumptions, used to derive the pseudos, affect predicted recovery in the simulations. Factorial experimental design (FED) is used to rank the various parameters. The impact of various assumptions used as part of the upscaling is also tested.

MODELLING HIERARCHY

In the SAIGUP modelling scheme, six facies associations were included to represent a shallow-marine system. For a full description of the large-scale modelling procedure and a description of the depositional system, see Howell *et al.* (2008). To apply the Geopseudo Method of upscaling, each facies association was modelled at appropriate scales (Fig. 1).

Lamina-set (metre-scale) models were built to capture lamina-scale effects on flow (see Table 1 for dimensions and parameters). These included trough cross-beds (TXB), hummocky cross-stratification (HCS) and planar bedding (PB) sedimentary structures. For a sedimentological description of the TXB and HCS models, see Daws (1992), Daws & Prosser (1992) and Corbett (1993). The modelling process is described in Yang & Stephen (2002) and Yang *et al.* (2004).

The TXB and HCS lamina-sets were modelled in three dimensions to capture anisotropy. The TXB were modelled deterministically and were periodic, while the HCS models were

Table 1. *Facies model parameters for the first level of upscaling*

Facies association	Facies model	N_x	N_y	N_z	L_x (m)	L_y (m)	L_z (m)	Low k (mD)	High k (mD)	Lamina thickness (cm)
OTZ	HCS 2D (OTZ_HCS)	100	1	200	0.5	0.5	0.1	10	50	0.5
LSF	HCS	40	40	50	0.5	0.5	0.1	50	150	2.0
LSF	HCS	40	1	40	0.5	0.5	0.1	50	150	2.0
LSF	HCS (LSF_HCS)	100	1	200	0.5	0.5	0.1	50	150	0.5
USF	TXB 3D (USF_TXB)	40	40	40	0.5	0.25	0.2	500	1500	0.5
USF	Planar bedding (USF_PB)	100	1	96	0.5	0.5	0.2	500	1500	0.208
CH	TXB (CH1_TXB)	40	40	40	0.04	0.04	0.02	50	150	0.075
CH	TXB (CH2_TXB)	40	40	40	0.1	0.1	0.05	100	300	0.15
CH	TXB (CH3_TXB)	40	40	40	0.2	0.2	0.1	200	600	0.25
CH	TXB (CH4_TXB)	40	40	40	0.5	0.5	0.25	400	1200	0.75
CH	TXB (CH5_TXB)	40	40	40	1.0	1.0	0.5	500	1500	1.25
CP	n/a	1000	1	1	75	n/a	n/a	n/a	40	n/a
OFF	n/a	1000	1	1	75	n/a	n/a	n/a	5	n/a

The term in brackets in the second (Facies) column corresponds to the terms in brackets in Figure 1. TXB models also have bounding surfaces which were 50mD for the USF_TXB models and 10, 20, 30, 40 and 50mD for CH1_TXB to CH5_TXB, respectively.

internally stochastic, but periodicity was guaranteed at the boundaries so that the structures were repeated. Tests showed that when upscaled, the resulting absolute and relative permeabilities were effectively isotropic for both facies. In addition, for HCS, there was negligible difference between three-dimensional models and two-dimensional random slices (results not shown). Coarse- (where cells were several cm in size, several times typical lamina thickness) and fine-grid models also produced similar results. What is important therefore is that numerical dispersion is compensated for correctly and flow connectivity captured accurately enough. This process depends on both the heterogeneity and the flow conditions. Planar beds consisted of horizontal laminae and were also modelled in two dimensions. Channels, which fine upwards, required decreasingly small TXB models and hence two stages of upscaling were applied to obtain the lamina-set pseudos. All lamina-set models were assumed to be a binary system of alternating high and low permeability, with the exception of TXB which contained a third, lowest, permeability representing set bounding surfaces.

Upscaled pseudos for these models were then applied to a second stage of upscaling using models representing flow within a simulation grid cell, which measured 75 × 75 × 4 m. At this scale, simulation cells for offshore transition zone (OTZ) and lower shoreface (LSF) facies associations were built from HCS models. The upper shoreface (USF) consisted of TXB overlying planar bedding. Channels consisted of layers, according to the fining-upwards sequence, with each containing TXB models of decreasing size and grain size. As a base case, the within-facies variability was ignored (i.e. between lamina-set as opposed to lamina-scale heterogeneity, which was captured at the smallest scale of modelling) and heterogeneity at the next scale represented average between-facies changes only.

The offshore and coastal plain facies associations were constructed from interbedded sands and muds. The sands, disk-like in reality, were assumed to be variable in length and homogeneous, while muds dominated the volume and typically have negligible permeability. Two-dimensional stochastic models were generated for a horizontal arrangement of three coarse cells. Sandbodies of variable horizontal length were placed randomly into a background of shale until a reasonable sand proportion was obtained. The proportion of sandbodies that connect over a distance, x, was determined and a connected volume and cross-section estimated. As vertical flow between sands was zero in these models, upscaling flow simulations were carried out in one dimension using the appropriate cross-sectional area after assessing connectivity in static models. For additional accuracy, three-dimensional models should be used to capture connectivity and tortuosity. It is unlikely, however, that these facies associations will affect flow significantly because the sand permeability is very low and flow is dominated by the background mud/shale. Reduced effort is therefore required for these facies association models compared to the channel, USF and LSF facies.

Petrophysics at the lamina scale

The flow simulations required input relative permeability and capillary pressure curves. These are often referred to as 'rock' curves, particularly when measured using special core analysis. Rather than use curves specific to one field, synthetic curves were adopted that could be related to the lamina-scale porosity and permeability (Corbett *et al.* 1992):

$$\phi = c_0 + m_0 log_{10}(k_{abs}), \tag{1}$$

$$S_{wc} = c_1 + m_1 log_{10}(k_{abs}), \tag{2}$$

$$S_{or} = c_2 + m_2 log_{10}(k_{abs}), \tag{3}$$

$$k_{rw}(S_w) = c_3(S_n)^{e_1}, \tag{4}$$

$$k_{ro}(S_w) = c_4(1 - S_n)^{e_2}, \tag{5}$$

$$P_c = c_5\sqrt{\phi/k_{abs}}(1 - S_{or} - S_w)^{e_3}/S_n^{e_4}, \tag{6}$$

where $S_n=(S_w-S_{wc})/(1-S_{or}-S_{wc})$ is the normalized water saturation. The base-case parameters (coefficients c_0–c_5, m_0–m_2, e_1–e_4) are given in Table 2. Water-wet curves were chosen in the base case as changes in wettability could not be represented systematically using the above equations. Capillary equilibrium was assumed as an initial condition so the same value of capillary pressure, 3 bars in the base case, is used at the minimum water saturation in all curves. The capillary pressure is zero at the residual saturation following the assumption of weakly water-wet rocks.

Fluid and rock properties

The suite of models considered in this paper simulates flow in a reservoir containing just light oil and water. For the fluid and rock properties, see Table 3.

Table 2. *Petrophysical variables assigned to equations (1)–(6) for the base case*

P_c			Saturation				Relative permeability				ϕ	
c_5	e_3	e_4	c_1	c_2	m_1	m_2	c_3	c_4	e_1	e_2	c_0	m_0
3.0	1.0	0.667	0.6	0.3	−0.165	0	0.3	0.85	3.0	3.0	0.2	0

BASE-CASE UPSCALING

The base case sought to capture the two-phase flow properties with a minimum but necessary set of assumptions. A saturation-dependent curve was required for oil and water relative permeability as well as capillary pressure for each facies association in the full-field model. These were obtained mostly using commercially available upscaling methods (Eclipse Manual 2003).

The Kyte & Berry method (1975) was used to calculate pseudos at all scales, with the exception of the three smallest Channel TXB models. At small scales, capillary pressure gradients dominate over viscous forces (Kortekaas 1985; Ringrose *et al.* 1993) and, therefore, the PCE method (Smith 1991; Pickup & Sorbie 1996) was used, where appropriate, with periodic boundary conditions.

The lamina-set models described above were assigned the parameters in Table 1. Pseudos for horizontal and vertical flow were obtained in all cases. For the Kyte & Berry method, the local fine-grid flow simulation model that was used to calculate pseudos consisted of three coarse cells aligned with the flow direction. This ensures that connectivity is represented accurately across the sedimentary structures. High permeability lamina-sets also required three coarse cells vertically when upscaling horizontal flow. A frontal advance speed of 0.3 m per day was assumed to be typical for both directions in the flowing part of the reservoir. For the PCE method, a single coarse cell with periodic boundary conditions was used. The upscaled absolute permeability values were obtained by pressure solution and inversion of Darcy's Law.

Base-case upscaling results

Absolute permeabilities for the upscaled facies models are shown in Table 4. To represent the flow from a physical perspective upscaled (pseudo) relative permeabilities and viscosities were converted into total mobility, M_{tot} and fractional flow, f_w, using:

$$M_{tot} = \frac{k_{rw}}{\mu_w} + \frac{k_{ro}}{\mu_o} \tag{7}$$

$$f_w = \frac{k_{rw}/\mu_w}{k_{rw}/\mu_w + k_{ro}/\mu_o} \tag{8}$$

The fractional flow is only strictly correct if capillary pressure and gravity effects are negligible but, in the above form, it allows assessment of the transport and breakthrough at the cellular level. The total mobility allows us to understand the bulk fluid flow, particularly the total flow rate and pressure.

The lamina-set pseudo total mobility and fractional flow curves (calculated from the pseudo-relative permeability curves) for horizontal flow are shown in Figure 2 for the channel facies and Figure 3 for the others. Vertical pseudos are not shown, although they were calculated and applied in the second level of upscaling.

The offshore and coastal plain models were upscaled only horizontally as they contain shales that are generally observed to be well connected, laterally. All other models were upscaled for x and z (upwards) flow. Table 5 shows the upscaled single-phase effective permeability for each facies association and these were consistent with the global statistics used in the full-field modelling (Matthews *et al.* 2008; Manzocchi *et al.* 2008*a*). The resulting pseudos for horizontal and vertical flow are shown in Figures 4 and 5, respectively.

Flow processes are affected by different forces at each scale and depend on the rock properties. At the fine scale, capillary pressures may dominate between wells and it was found that the saturation increased more quickly in lower permeability laminae, particularly those in small sedimentary structures, and where low flow speeds were modelled. In most of the lamina-set models, however, the front was still reasonably well defined such that some compensation for numerical dispersion was required. This effect can be seen in the pseudo-mobility curves which show late breakthrough times for grid cells at the intermediate scale (Figs 2, 3). At the second scale, capillary forces also played a part in reducing gravity segregation in poorer quality facies. The resulting front was more vertically aligned than in those facies of higher permeability and compensation for numerical dispersion was again required (Fig. 4). Note that the computed breakthrough saturation for each facies lies between 0.55 and 0.6 (Figs 4b, 5b) but each facies has an initial saturation that decreases with increasing average permeability. In the full-field models, flow was dominated by the high permeability upper shoreface and channel facies.

Limitations of the base-case assumptions

During calculation of the base-case pseudos a number of potentially important features were ignored. At the small scale,

Table 3. *Fluid and rock properties used at all scales*

	Formation volume factor (reservoir m^3/stock tank m^3)	Viscosity (cP)	Density ($kg\ m^{-3}$)	Compressibility (bar^{-1})
Oil	1.5	1.0	721	0.0001
Water		0.4	1000	0.00001
Rock				0.00001

Table 4. *Upscaled effective permeabilities calculated by pressure solution for the lamina-set models in Figure 1*

Facies Association	Facies	Effective permeability (mD)		
		k_x	k_y	k_z
OTZ	OTZ_HCS	21.5	21.5	16.5
LSF	LSF_HCS	84.0	84.0	74.4
USF	USF_TXB	660	654	287
USF	USF_PB	1000	1000	750
CH	CH1_TXB	69.6	72.5	42.8
CH	CH2_TXB	139	145	85.5
CH	CH3_TXB	273	279	147
CH	CH4_TXB	528	523	230
CH	CH5_TXB	660	654	288

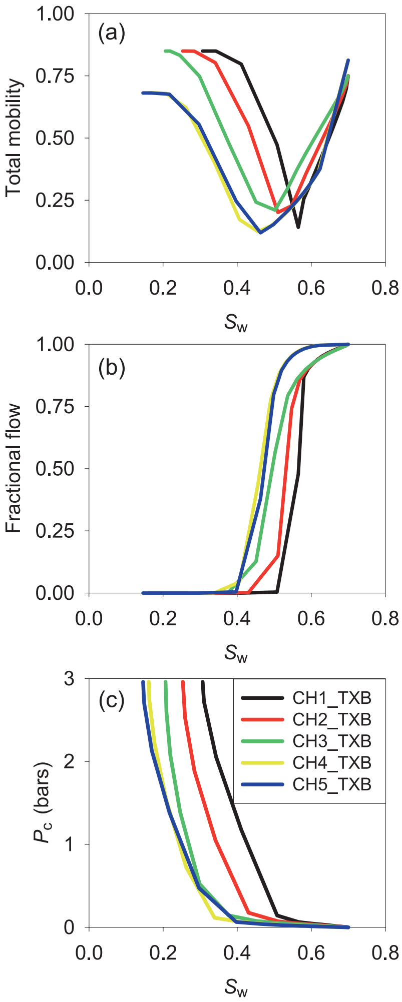

Fig. 2. Upscaled (**a**) total mobility, (**b**) fractional flow and (**c**) capillary pressure for the bed-scale models of CH_TXBs. The legend in (c) applies to (a) and (b). See Figure 1 and text for details.

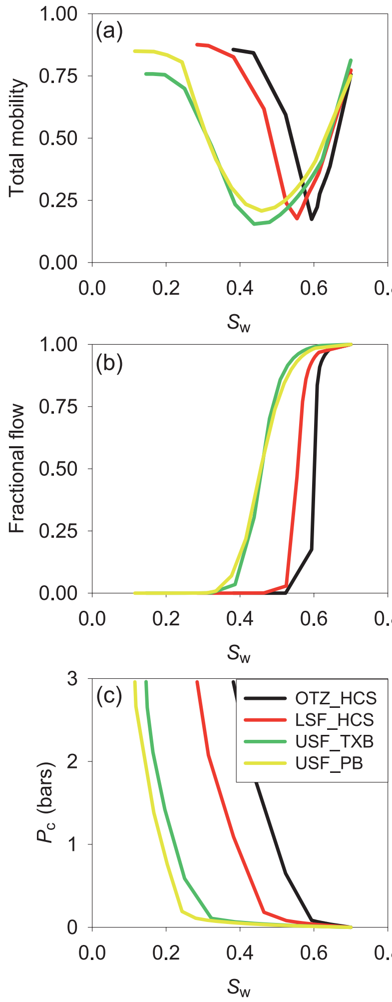

Fig. 3. Upscaled (**a**) total mobility, (**b**) fractional flow and (**c**) capillary pressure for the OTZ_HCS, LSF_HCS, USF_TXB and USF_PB models. The legend in (c) applies to (a) and (b). See Figure 1 and text for details.

two lamina permeability values were used in most cases. In reality, laminae properties vary, depending on sediment supply and sorting, potentially requiring a population of upscaled facies models of varying upscaled permeability and pseudo-properties. It is also likely that the input petrophysical properties vary to reflect variation in pore-size distributions and connectivity, grain size and wettability.

At the larger scale, within-facies variability should also be considered, including spatial correlation. Further, the full-field geological models were created at an intermediate scale (37.5 × 37.5 × 1 m, Howell *et al.* 2008). These were upscaled for static properties only, after which the pseudos were applied. As a result, the grid cells of the final upscaled model contain amalgamated facies associations. In practice, only the most dominant facies association by volume is used to allocate the pseudo. For accuracy, these should be upscaled individually, although this would yield unique pseudos for each simulation cell. Grouping of pseudos (e.g. Dupouy *et al.* 1998) or perhaps end-point scaling of typical relative permeabilities could be applied, though this also increases the workload significantly.

The flow conditions assumed in the base case are unlikely to apply over the reservoir, particularly the local boundary conditions that were used, including both pressure and fractional flow. A single horizontal flow velocity was assumed to determine each pseudo at the facies association scale and the fractional flow was controlled by pseudo-wells applied to a skin of grid cells surrounding the upscaled volume. In reality, the flow velocity will vary in magnitude and direction throughout the reservoir, depending on proximity to the wells, connectivity etc. Direction- and speed-dependent pseudos should be calculated, perhaps with different speeds in each direction. The fractional flow may also vary, depending on the source of invading water. A predominantly horizontal flow in a region of low or moderate permeability may see gravity-induced water invasion after an overlying high permeability layer has been

Table 5. *Upscaled absolute permeabilities obtained using the Pseudo package in Eclipse for the simulation grid cells*

Facies association	Effective permeability (mD)		
	k_x	k_y	k_z
OFF	0.06	0.06	0
OTZ	21.4	21.4	0
LSF	84.0	84.2	71.6
USF	745	740	339
CP	2.72	2.72	0
CH	391	391	124

Facies are identified by initials and correspond to the terms in square brackets in Figure 1. Intermediate-scale models contained grid cells that were 0.5 × 0.5 × 0.1 m and measured 75 × 75 × 4 m in total.

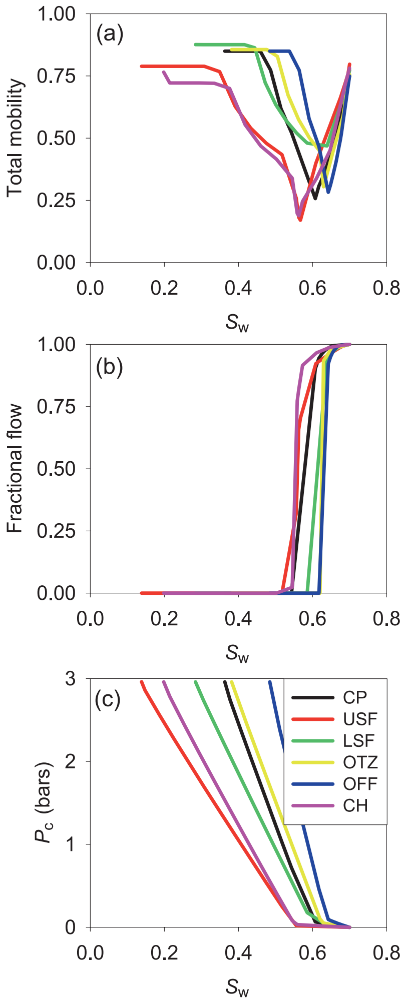

Fig. 4. Base-case upscaled (**a**) total mobility, (**b**) fractional flow and (**c**) capillary pressure obtained for horizontal flow and applied to the six facies associations modelled at the full-field scale. The legend in (c) applies to (a) and (b). See Figure 1 for facies names.

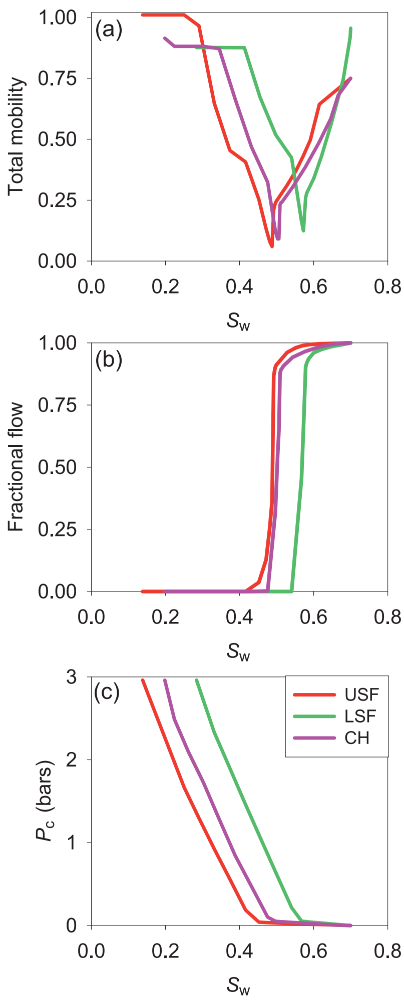

Fig. 5. Base-case upscaled (**a**) total mobility, (**b**) fractional flow and (**c**) capillary pressure obtained for vertical flow and applied to the USF, LSF and CH facies associations at the full-field scale. The legend in (c) applies to (a) and (b).

swept. This would seriously affect the outcome from upscaling. In addition, successive upscaling across several scales using a dynamic method, such as Kyte & Berry (1975), can overcompensate for numerical dispersion (Christie *et al.* 1995) because pseudos are generally calculated using a small local grid. This may be avoided by upscaling the lamina-set models using the PCE method. Stephen *et al.* (2003) have shown that this is more accurate for 1D horizontal models at least.

Finally, weakly water-wet relative permeability curves were assumed so that capillary trapping could not occur. More likely, in mixed wet reservoirs, capillary pressure curves for water displacing oil show a negative (drainage) leg indicating that large pores are oil-wet. This would affect our estimate of capillary trapping effects.

UNCERTAINTY ANALYSIS

Reducing the small-scale parameter space

Prior to this study, a pilot study was carried out, primarily to reduce the parameter space describing the geological models and the petrophysical properties (for full details see Yang & Stephen 2002 and Yang *et al.* 2004). The effect of parameters on capillary trapping and also on the shape of pseudos after upscaling TXB and HCS models using the PCE method was examined. These pseudos were then used in simulation models at the next scale of upscaling where the effect on production rates and water cut were examined. It was found that the lamina-scale permeability contrast (expressed as the coefficient of variation, C_v, over each model) and the shape of the capillary pressure curve (e_4 in equation (6)) were the two most important parameters, though others could be important.

It was subsequently decided to vary these two parameters in the analysis presented here to determine how upscaling affects predictions in our full-field models. In the base case, the same C_v was used throughout the lamina-sets, with the exception of the OTZ (see Table 6). It was then assumed that this parameter would vary by the same degree throughout the facies associations.

Parameters and methods

Table 7 summarizes the parameters and methods considered.

Table 6. *Fine-scale properties used for minimum, mean and maximum values in the analyses*

Parameter	Low	Base case	High
C_v (OTZ_HCS)	0.367	0.667	0.933
C_v (other models)	0.2	0.5	0.8
e_4	0.4	0.667	1.0

Table 7. *Sensitivity variables that were used during the factorial experimental design A and B analyses shown in Figures 11 and 12*

Parameter	Values in factorial experimental design A	Element of P B	In Figures 11–12
Aggradation angle	Low, high*	Low, high	1
Clinoform barrier strength	Low, high*	Low, high	2
Shoreline curvature	Low, high*	Low, high	3
Shoreline parallel faults	Unfaulted, faulted	Unfaulted, faulted	4
Shoreline perpendicular faults	Unfaulted, faulted	Unfaulted, faulted	5
First stage upscaling	PCE or PVW	PCE or PVW	6
Upscaling flow direction	X or X and Z	X	7
Small-scale C_v	Low, high (see Table 5)	Medium	8
P_c exponent	Low, high (see Table 5)	Medium	9
Upscaling flow speed	0.3 m s^{-1} only	0.03 and 3 m s^{-1}	10

*For definition see Howell *et al.* (2008)

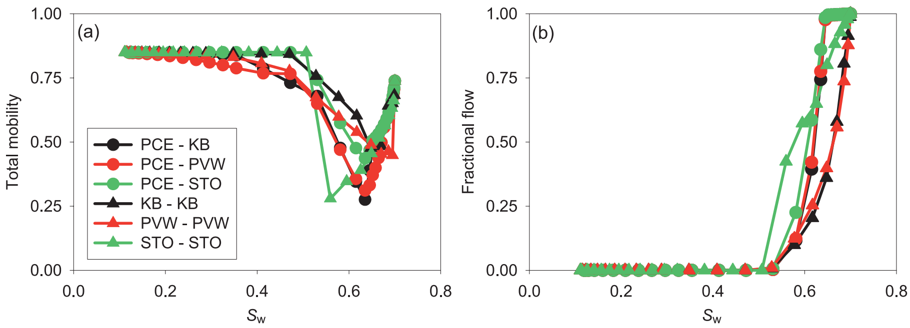

Fig. 6. Example large-scale pseudos for (**a**) total mobility and (**b**) fractional flow (for the USF) showing the effect of different upscaling methods at each scale. Abbreviations for the methods are provided in the nomenclature and abbreviation table. In the legend the first method was applied at the bed scale and the second method at the simulation cell scale. The legend applies to (a) and (b).

- **Large-scale sedimentological parameters.** Simulations were based on full-field coarse-scale models, constructed to explore combinations of the sedimentology parameters for aggradation angle, curvature of the shoreline and clinoform barrier strength from minima to maxima (see Howell *et al.* 2008). All eight combinations of minimum and maximum parameter values were used as well as a model with all parameters set to a middle value. Manzocchi *et al.* (2008*a*) show the subset of nine large-scale sedimentological models used in the current analysis.
- **Large-scale structural parameters.** Four structural models were used representing unfaulted, shoreline-parallel, shoreline-perpendicular and compartmentalizing fault systems. The faults were modelled using the highest fault density level considered elsewhere, and using a relatively permissive fault-rock permeability model (referred to elsewhere as model 2). Further details are given by Manzocchi *et al.* (2008*b*).
- **Small-scale parameters.** These included the permeability variation C_v and the capillary pressure exponent, e_4, in equation (6).
- **First stage upscaling method.** Rather than use the same dynamic method of upscaling at the first and second stages, the PCE method was used as a faster and often more reliable alternative at the first stage. Figure 6 shows that when using the PCE method followed by the K&B method, the final pseudos show less compensation for numerical dispersion. In the USF model, the first stage upscaling method alters the shape of both total mobility and fractional flow, although the breakthrough saturation is the same.
- **Second stage upscaling method.** Stone's method (STO) and the PVW method were applied at the second stage. Figure 6 shows the effect of upscaling method on the pseudos. For a full discussion of the methods, see Barker & Thibeau (1997). The K&B method inverts Darcy's Law using an average pressure calculated from the central column in a coarse cell, weighted by relative permeability, permeability and cell thickness. The PVW method is essentially the same except that, instead, pressures are averaged over the whole cell and weighted by pore volume. Stone's method, on the other hand, calculates an average mobility and fractional flow at the coarse cell interface. All three methods usually give the same saturation at which water becomes mobile in the coarse cell in more viscous-dominated floods. The slow flow rate USF model is more gravity dominated and the Stone method gives different results and is known to perform less well in such circumstances. The capillary pressures were upscaled based on the same fine-scale simulation data, using pore volume weighed pressures (Eclipse Manual 2003) and gave the same pseudo-curve in each case.
- **Directional pseudos.** As a base case, the full-field simulations in the SAIGUP project were based on isotropic pseudos for horizontal flow only. The vertical pseudos were included as part of this analysis to determine whether the anisotropy of the fine scale and the flow direction are important.
- **Speed-dependent pseudos.** The effect of flow speed was investigated where one speed is assumed everywhere in the reservoir. Figures 6–8 show the effect of varying the speed. Capillary effects appear to be stronger in the low permeability models at the small scale, while at larger scales and in high permeability models, gravity effects dominate. At the base-case frontal advance speed of 0.3 m per day, the pseudos reflect a mixture of gravity and viscous forces. Gravity has the strongest effect at 0.03 m per day (Fig. 7) while, at 3 m per day (Fig. 8), the flow is viscous dominated and compensation for numerical dispersion is required. For each upscaling method, the pseudo-relative permeabilities for oil are quite similar at low rates but not for water. The capillary pressure curves (Fig. 9) show distinct flow speed effects.

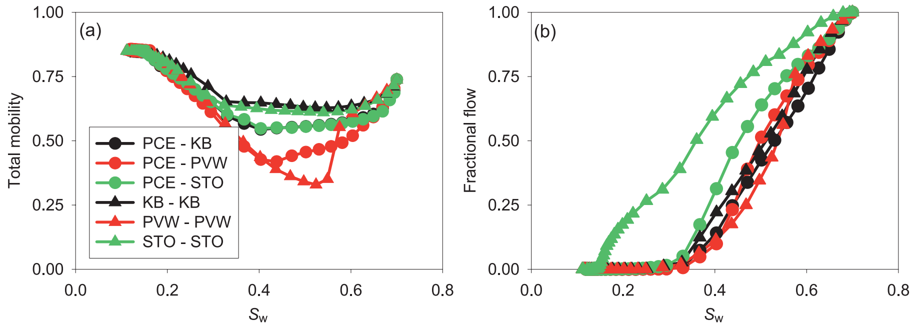

Fig. 7. Example large-scale pseudos for (**a**) total mobility and (**b**) fractional flow (for the USF) showing the effect of different upscaling methods at each scale. Pseudos as in Figure 6 except that the induced flow velocity was 10% of the base case. Abbreviations for the methods are provided in the nomenclature and abbreviation table. In the legend the first method was applied at the bed scale and the second method at the simulation cell scale. The legend applies to (a) and (b).

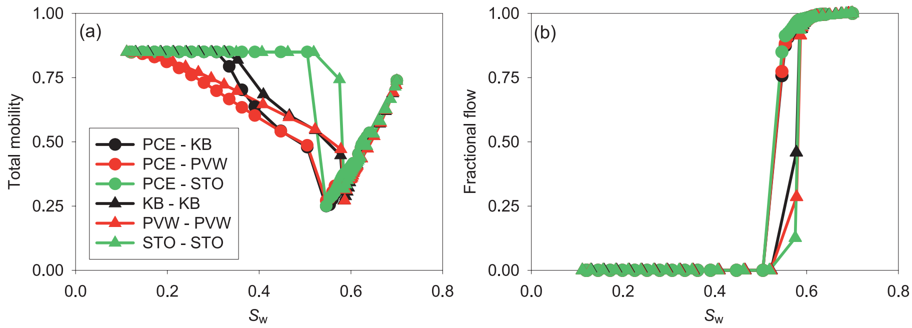

Fig. 8. Example large-scale pseudos for (**a**) total mobility and (**b**) fractional flow (for the USF) showing the effect of different upscaling methods at each scale. Pseudos as in Figure 6 except that the injection rate was 10 times the base case. Abbreviations for the methods are provided in the nomenclature and abbreviation table. In the legend the first method was applied at the bed scale and the second method at the simulation cell scale. The legend applies to (a) and (b).

FULL-FIELD SIMULATION RESULTS

The full-field simulation models are described more fully in Matthews *et al.* (2008) including well locations and controls, PVT data and other fluid properties. In the simulations described a well design optimized for an unfaulted reservoir was used. Figure 10 shows the production rate profiles for a sub-sample of models with varying large- and small-scale parameters, as well as upscaling methods. The results are similar to those found by Skorstad *et al.* (2008) which focused on the effect of large-scale geological parameters only.

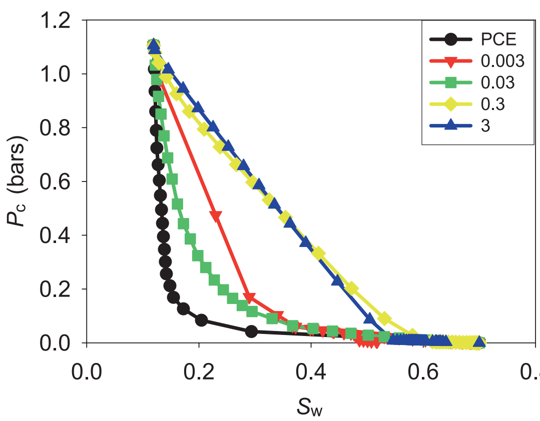

Fig. 9. Flow speed dependence of the upscaled capillary pressure curve. The legend indicates the frontal advance speed (m per day) used to control the flow. The PCE method assumes zero flow velocity.

Factorial experimental design (FED)

A two-level full factorial experimental design (FED) analysis was applied to rank first-order single and multi-parameter interaction effects. Similar methods were applied previously in petroleum engineering to determine the impact of various parameters on field development (Damsleth *et al.* 1992; Peng & Gupta 2003), the impact of geological parameters on production variables for both single-scale models (White *et al.* 2000, White & Royer 2003) and across various scales (Opdal & Kossack 1990; Jones *et al.* 1995). White *et al.* (2000) suggested that a quadratic model should be used in general. However, this would increase the number of simulations required for continuous variables.

The FED here assumes a response surface that is linearly dependent on parameters and their products (Box & Hunter 1961; Box *et al.* 1978; Yang *et al.* 2004). The set of simultaneous linear equations (see Appendix B) can then be inverted. The study assumed minimum and maximum values for continuous parameters, while categorical parameters such as upscaling method, directionality etc. were varied in a binary format.

The equation to be solved is written in terms of the limits of our parameters. If equation (B1) is applied using a mean of the limits for one parameter, all terms including that parameter are zero. Thus, for an *N*-dimensional parameter space, if an *N-P* FED (i.e. 2^{N-P} simulations) with *P* parameters set to the mean value is run, the coefficients for all parameters that are varied will be obtained. A second FED can then be run with *N-Q* parameters (*Q* are set to their mean value and are different from the original *P*), extending knowledge of the coefficients. The coefficients involving parameters varied in both FEDs should

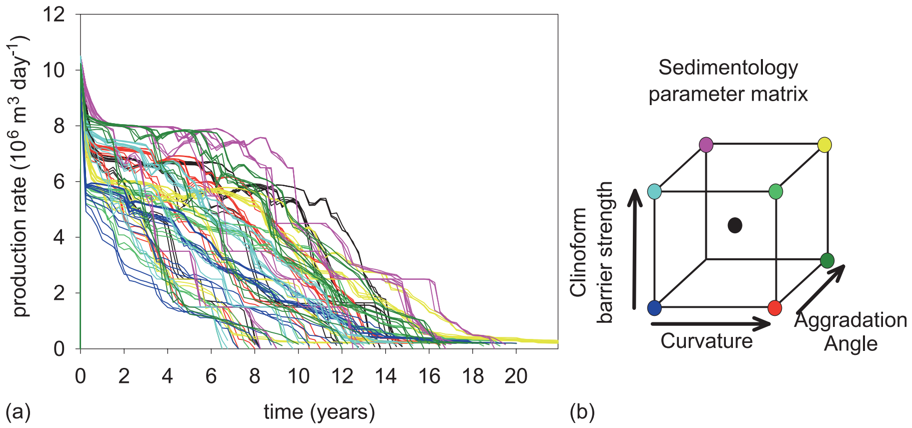

Fig. 10. (**a**) Oil production rate for a number of models and (**b**) sedimentology parameter matrix. The models in (a) consist of different combinations of the sedimentology parameters, small-scale parameters and second stage (facies association to grid cell) upscaling methods. The sedimentology settings are indicated in (b). The medians and all combinations of minimum and maximum values of e_4 and C_v of permeability (Table 6) were used. All three upscaling methods (K&B, STO and PVW) were used at the second stage. The PCE upscaling method was used at the first stage, the pseudos were calculated for a flow speed of 0.3 m per day and horizontal pseudos were used. Line colours in (a) indicate the strength of the three sedimentology parameters as shown in the sedimentology matrix.

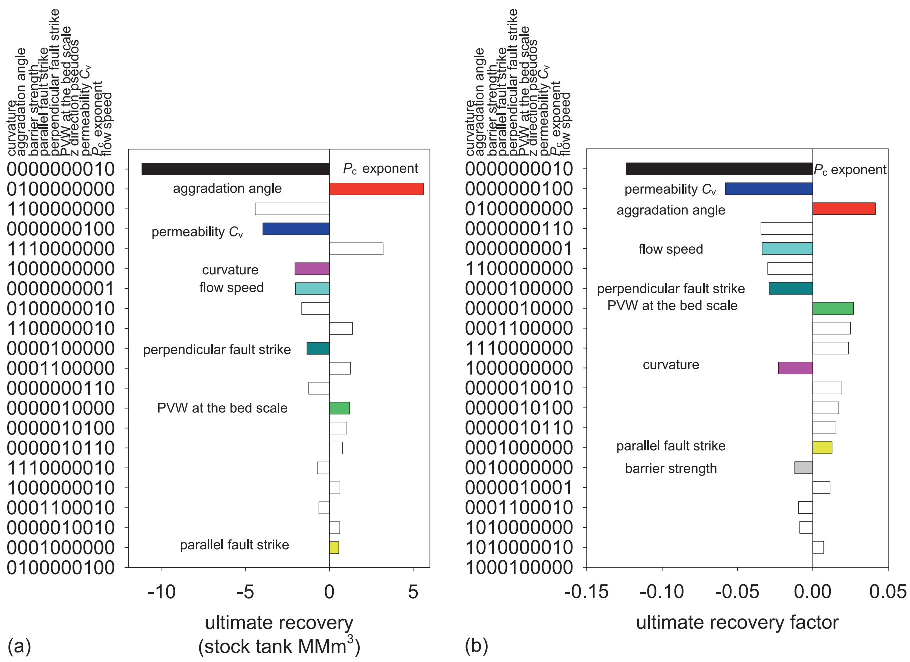

Fig. 11. Factorial experimental design (FED) coefficients for ultimate (**a**) recovery and (**b**) recovery factor after merging results from FEDA and FEDB. Single parameter effects are indicated by the colours and the same colour scheme is used in Figure 12. Ones in the binary numbers labelling the bars indicate which parameters are interacting in equation (B2) in Appendix B. A single one indicates a single parameter effect while multiple ones indicate interaction terms.

be the same if the equation is valid. All coefficients are obtained except those that involve interactions between parameters from both of the *P* and *Q* groups. This is computationally cheaper than a full FED.

In the study there are ten parameters and, to reduce the number of simulations, two analyses (FEDA and FEDB) were carried out, where nine and seven parameters were varied, respectively (see Table 7). Six parameters were varied in both studies and it was found that their coefficients were strongly linearly correlated. Those from FEDA were about 10% larger, so the extra coefficients gained from FEDB were scaled using the linear correlation. All available coefficients for ultimate cumulative recovery and for recovery factor were plotted (Fig. 11). Note that although the single parameter coefficients for e_4, C_v, flow speed and direction were obtained, it is not possible to tell how flow speed or direction interact with either e_4 or C_v. Also, flow direction is a categorical variable, so there is no mean. However, its effect for ultimate oil recovery was negligible in FEDA.

Capillary pressure exponent e_4 is the dominant parameter for both recovery and recovery factor, while C_v of permeability at the fine scale is third and second in importance, respectively. The flow speed is also moderately important, while the use of the PVW method at the bed scale affects recovery factor, but ultimate recovery only to a small degree. Capturing the vertical pseudos is not important at all. The parameters e_4, C_v and flow speed all influence the gradient of capillary pressure with saturation. A steeper capillary pressure curve leads to a reduced STOIIP. The end points of the relative permeability curves decrease with increasing C_v which further influences STOIIP.

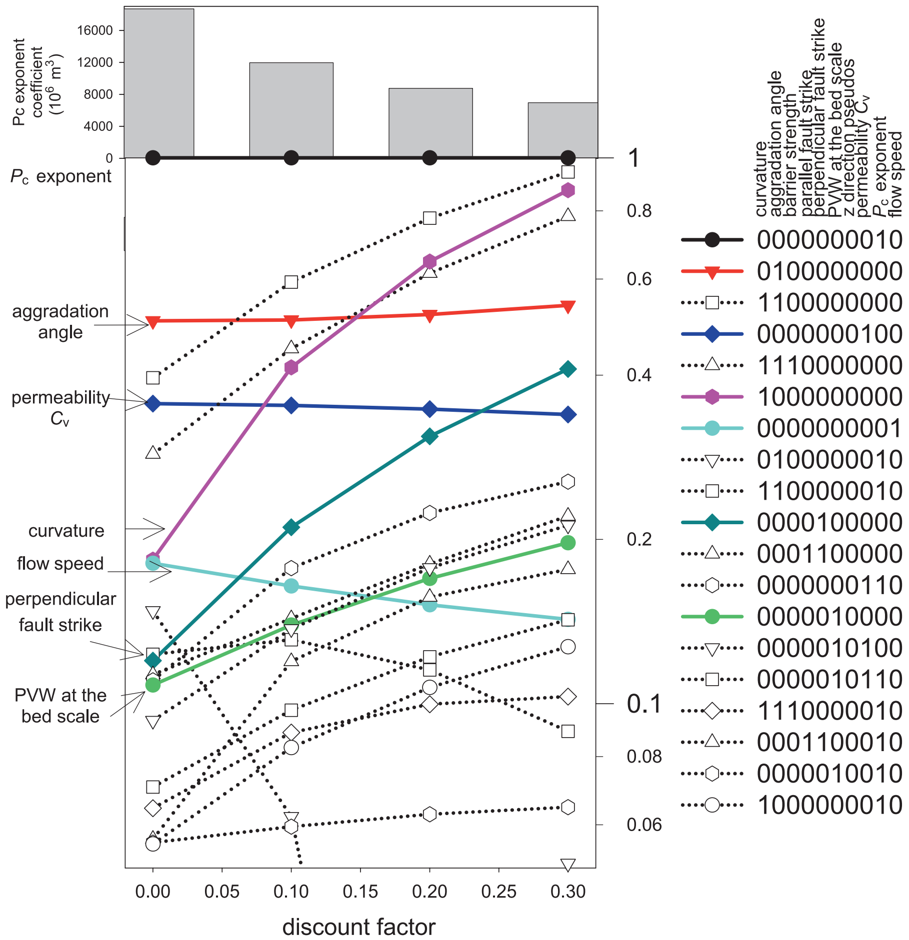

Fig. 12. Absolute value of the factorial experimental design (FED) coefficients, normalized by the coefficient of the P_c exponent, raw values of which are shown in the bar plot on top. Single parameter interactions are indicated with arrows and the colours correspond to those used in Figure 11 for each parameter. Multiple parameter interactions are indicated by dotted lines and empty symbols. Note that the coefficients have been plotted on a log scale and only the 19 most important are shown.

Thus, e_4 and C_v strongly affect the STOIIP and hence ultimate recovery. An increased transition zone can also lead to improved connectivity of mobile water so that early breakthrough occurs leading to reduced recovery factor. By switching from the PCE to the PVW upscaling method at the bed scale, the breakthrough time in the grid cells was increased, thus improving both recovery factor (significantly) and ultimate recovery. The results for the large-scale sedimentological and structural parameters found are complementary to those reported by Skorstad *et al.* (2008).

FEDA and FEDB were repeated on discounted value calculated from:

$$V = \int_0^{30} \frac{R(t)}{(1+d)^t} dt \qquad (9)$$

where $R(t)$ is the production rate, d is the discount factor. This enables weighting of the predicted recovery towards early production-time but also allows a more appropriate economic assessment of the impact of the various parameters. Discount factors of 0.1, 0.2 and 0.3 were investigated. The resulting change in parameter effect coefficients is shown in Figure 12. The coefficients were normalized by the coefficient for the P_c exponent.

The capillary pressure exponent is the most important parameter although it does become relatively less important with increasing discount. Aggradation angle and the permeability properties decline in relative importance slightly while the shoreline curvature effect increases, including its multi-parameter interaction with the other two sedimentological parameters. In absolute terms the effect of curvature is unaffected by increasing the discount factor. The impact of assumed flow speed decreases in importance with increasing discount such that it falls below the bed-scale upscaling method.

The changes in the importance of the parameters as discount increases reflects how each parameter impacts on oil recovery over the production period. Parameters that dominate early on in production time, perhaps by altering the breakthrough time, have less impact later on. Curvature is one of these, together with the bed-scale upscaling method. Other parameters generally decline in both relative and absolute importance. The effect of the capillary pressure exponent, C_v of permeability and flow speed all affect later production, not just breakthrough.

Upscaling analysis

To quantify the effect of the choice of upscaling method and associated assumptions, a number of simulations were run with different parameters; the results of a simpler upscaling assumption (usually the base case) were compared to one that was more elaborate using the following metrics:

- **root mean sum of squares of differences** (RMS) calculated over the production rate time series:

Table 8. *List of combinations of parameters considered in the upscaling analysis shown in Figure 13*

No.	Large-scale upscaling	Small-scale upscaling	Directional pseudos	Velocity (m per day)	Small scale (C_v and e_4)[a]
1	K&B vs. PVW	PCE	X	0.3	Low and high
2	K&B vs. STO	PCE	X	0.3	Low and high
3	PVW vs. STO	PCE	X	0.3	Low and high
4	PVW	PCE	X vs. X+Z	0.3	Low and high
5	PVW	PVW	X vs. X+Z	0.3	Low and high
6	PVW	PCE vs. PVW	X	0.3	Low and high
7	PVW	PCE vs. PVW	X+Z	0.3	Low and high
8	PVW	PCE	X+Z	0.3 vs. 3.0	Med
9	PVW	PCE	X+Z	0.03 vs. 0.3	Med
10	PVW	PVW	X+Z	0.3 vs. 3.0	Med
11	PVW	PVW	X+Z	0.03 vs. 0.3	Med

[a]Small-scale properties comprise either the median set of parameters or the full range with all combinations of min and max as well as the median.

$$RMS(\underline{R}^s - \underline{R}^e) = \frac{1}{N}\sum_{i=1}^{Nt}(R_i^s - R_i^e)^2 \qquad (10)$$

where R_i is the production rate at the i^{th} time step and superscripts s and e refer to the simplified and elaborate upscaling assumptions and N is the number of time steps over which production occurs (or 20 years whichever is smaller). This is analogous to the approach taken in history matching and provides an absolute measure, averaged over production time.

- **normalized RMS** (NRMS) calculated over the production time:

$$NRMS = \frac{2RMS(\underline{R}^s - \underline{R}^e)}{RMS(\underline{R}^s) + RMS(\underline{R}^e)} \qquad (11)$$

- **normalized maximum difference** (NMD) calculated to account for differences in cumulative volume produced, V_i, giving a more obvious and meaningful variable. Normalization to the final volume produced was applied to give a relative measure:

$$NMD = \frac{max\,|\,V_i^s - V_i^e|}{max(V_i^s)} \qquad (12)$$

Equation (12) can also be applied to production rates with the maximum for oil obtained at t=0.

A number of different upscaling assumptions were investigated:

- upscaling algorithm at the large scale (K&B vs. PVW vs. STO);
- upscaling algorithm at the small scale (PCE vs. PVW);
- isotropic vs. anisotropic pseudos (i.e. same assumed flow direction when upscaling);
- upscaling flow speed (slow vs. medium vs. fast).

Table 8 describes 11 different sets of models that were grouped for study. In each set several parameters were varied. Figure 13 shows the statistics (mean and spread of both difference measures described above) for each set. NMD, RMS and NMRS results were qualitatively very similar throughout and correlated linearly on a log-log scale. NMD and RMS distribution plots are very similar to those in Figure 13.

The large-scale upscaling method was investigated in sets 1 to 3. For small to medium values of the P_c exponent and the C_v of small-scale permeability, the NMD upscaling difference was less than 0.01. Larger values of these parameters increased differences up to a maximum of 0.1. The main cause of the differences is due to the way that each method captures fine grid changes in fluid mobility, especially prior to breakthrough in the coarse cell. Post breakthrough, the pseudo-relative permeabilities are very similar for both water (Figs 6–8) and oil (even when viewed on a log scale – data not shown). The PVW and K&B methods depend on weighted averages of the fine grid pressure, which is dependent on fine grid mobility. In addition, the weighting used in the K&B method also depends on the relative permeability. Stone's method, on the other hand, uses only fine grid mobility at the edge of the coarse cell and does not use pressure at all. The result is that, pre-breakthrough, the pseudo-relative permeability for oil is lowest using the PVW method and largest using Stone's method, where it is constant with saturation until breakthrough. At the full-field scale, mobility is therefore changed, resulting in different pressure and flow rate distributions. The effects of upscaling are apparent at large values of P_c exponent, e_4 and C_v of permeability at the small scale because more cells lie in the transition zone, have more mobile water and thus the mobility is different. For most cases, however, the choice of large-scale upscaling algorithm is not very important, except in a small number of cases, most of which have capillary effects which are extreme rather than typical.

Sets 4 and 5 determined whether anisotropy of the pseudos would affect results when using either the PCE or PVW methods at the first stage of upscaling. In the base case, pseudos obtained for horizontal flow were used for flow vertically between grid cells in the full-field model. A more appropriate approach would be to calculate pseudos using fine-grid

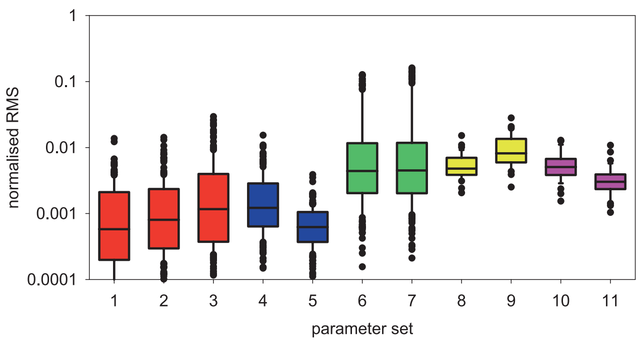

Fig. 13. Variation in the effect of different upscaling approaches (see Table 7 for details of each parameter set) showing normalized RMS distributions. Note that the y-axes are in log scale. The box plots indicate 25th and 75th percentile by the box, 10th and 90th percentile by the whiskers, and points outside of these are shown as symbols. The colours indicate that similar upscaling effects were analysed.

simulations of flow horizontally and vertically, which results in anisotropic pseudos. The range of differences due to anisotropy was similar to the results for set 3, indicating a similar average level of importance but with narrower spread. The PCE pseudos at the fine scale were less anisotropic than those obtained using the PVW method so the former's impact was reduced. The strongest effects occurred in models with high e_4 and C_v.

In sets 6 and 7, the effect of the first stage upscaling method was analysed for cases where anisotropy was ignored or included in the pseudos. The effect of using the PCE upscaling method at the fine scale was compared to the PVW method and the range of differences was significantly larger for both sets compared to sets 1–5. The largest differences occurred when C_v and e_4 were both large and were due to the reservoir approaching an uneconomic limit early in production time because of the earlier breakthrough that results from using the PCE pseudos. This effect was largest when PCE pseudos were used because the early breakthrough that occurs both from having more mobile oil and the pseudos was combine.

Finally, the effect of flow speed was considered (sets 8–11), resulting in an almost constant difference regardless of small-scale upscaling method. Again, the pseudo-capillary P_c curve is important, leading to large differences in the shut-in times of wells due to economic constraints. These differences are mostly apparent late in the production life of the reservoir and pseudos calculated at slow rates give more optimistic estimates of total production than fast rates.

DISCUSSION

This study was begun with two aims. First, a set of facies association-dependent relative permeability and capillary pressure saturation functions was required that would suitably represent the small-scale flow physics in a shallow-marine reservoir. These were obtained with minimum but necessary assumptions, such that lamina-scale heterogeneity and the effect it has on initial and final saturations and on the shape of the flow functions were represented. Adhering to more general conditions (e.g. variable flow speed, direction, etc.) would have increased model complexity and therefore CPU time, leading to a reduction in the parameter space that could be investigated. The second part of the study aimed to quantify the implications of those assumptions relative to the full SAIGUP study.

The analysis shows that for cumulative production, the small-scale parameters are first and third in order of importance. Both strongly determine the shape of the capillary pressure curve. This property determines the initial saturation distribution and hence the STOIIP and connected flow paths for water. The second most important parameter was the aggradation angle and there were important interaction effects with either, or both of, the curvature (fifth, individually) and clinoform barrier strength parameters (ninth individually and potentially negligible). Flow speed was fourth in importance, indicating that the balance of forces must be accounted for adequately when upscaling. Perpendicular alignment of the faults to the shoreline was sixth in importance individually, while the parallel alignment was eighth (potentially negligible). These fault-specific sensitivities were found using relatively permeable fault rocks and are similar to the effects of fault juxtaposition observed by Manozcchi *et al.* (2008*b*). Had less permissive fault-rock properties been considered then faults would be more important, particularly interactions of the two orientation models, since inclusion of both is required for converting a non-compartmentalized reservoir into a compartmentalized one.

The upscaling method at the small scale (PVW or PCE) was of some importance. An obvious observation was the absence of the effect of anisotropy of pseudos, particularly when considering upscaling differences. This is not too surprising since much of the movement of fluids occurred in the best quality sands (USF and channels) and the flow was therefore predominantly horizontal. In a bottom drive-dominated reservoir, the vertical pseudos would have more importance.

The impact of the upscaling was examined using three measures. The analysis did not consider the truth case, where a fine-grid simulation is run to consider the real upscaling error. This was impossible, given the number of grid cells required. However, the effect of different methods was compared. Geoscientists and engineers are often in a position where they have to choose a method and the impact of making that choice arbitrarily needs to be known. It was found that neither the upscaling algorithm at the coarse scale nor anisotropy of the pseudos were important (except for large e_4 and C_v). When considering the upscaling method at the small scale, the small-scale properties (P_c exponent, e_4 and C_v) could affect the choice of method. The effect of flow speed was independent of parameters, however, and consistently important throughout.

Previously (Pickup & Stephen 2000), it was found that the PCE method could be applied to give reliable pseudos with fewer of the problems associated with dynamic pseudos. Of course, if capillary trapping is evident, then a dynamic or mixed steady state method may be more appropriate. This study found that the PVW and PCE methods gave similar results, except in combinations of extreme e_4 and C_v of permeability. It is, therefore, recommended that the PCE method be applied at the smallest scale (provided an appropriate second level of upscaling is used) for speed and to improve the calculation of pseudo-capillary pressure. Horizontal pseudos need not be calculated only while the flow rate is more important and can be captured at the large scale. At the larger scale, the PVW should be used (following Barker & Thibeau 1997).

Upscaling may succeed or fail, depending on whether or not the boundary conditions of the upscaled model match those of the reservoir. Perhaps the most important boundary condition is the flow velocity. This work found that speed is very important, while direction is less so. The speed affects the balance of forces at the fine scale (Stephen *et al.* 2001) and varies throughout the reservoir. Further work is desirable to account for flow speed more accurately. An initial pressure solution could be used to determine flow rates throughout the model and then rate-dependent pseudos could be applied appropriately. The poorer quality facies associations will probably experience a slower flow speed, enabling more effort to be spent on the pay zones. Saturation upscaling of the geological model should also be used to scale pseudos for different facies. This would better capture the within-facies association variation as well as facies amalgamation. In addition to the speed, the fractional flow at the boundary of the upscaled model must be captured. This represents one of the more difficult aspects to get right in upscaling and can render pseudo-relative permeability curves useless. Finding the right boundary conditions can be very difficult, requiring many fine-scale pseudos to be calculated.

Finally, a capillary pressure model was chosen that represented a water-wet medium such that capillary pressure was zero when the residual oil saturation was reached. Capillary trapping in water-wet systems can occur when the capillary forces are strong in small-scale highly heterogeneous sedimentary structures, giving a low final water saturation. Alternatively, a mixed wettability may have been more accurate and would have altered the initial saturation distribution. However, the equations did not allow for changes in wettability as a function of rock quality in a consistent manner.

CONCLUSIONS

Using a two-level full factorial experimental design analysis, this study has investigated the effects of upscaling and fine-scale parameters on reservoir production from a suite of synthetic shallow-marine reservoirs. The principal findings of our analysis are:

- the five most important parameters were P_c exponent, aggradation angle, permeability C_v, assumed flow speed and shoreline curvature;
- fault direction (perpendicular and parallel to the shoreline) and the small-scale upscaling method were of moderate to low importance;
- sedimentological barrier strength and the direction of flow considered when upscaling were unimportant;
- shoreline curvature became more important for higher discount levels;
- choice of upscaling algorithm and anisotropy of the pseudos were not very important (unless C_v and e_4 were large), whereas accounting for the flow speed during upscaling was.

APPENDIX A: NOMENCLATURE AND ABBREVIATIONS

Table A1. *Nomenclature*

C_v	Coefficient of variation
c_i	Coefficients in equations (1)–(6)
d	Discount factor
e_i	Exponents in equations (1)–(6)
f_w	Fractional flow (ignoring capillary and gravity effects)
k_{abs}	Permeability (mD)
k_{ro}	Oil relative permeability
k_{rw}	Water relative permeability
m_i	Gradients in equations (1)–(6)
M_T	Total mobility (mD/mD/cP)
P_c	Capillary pressure (bar)
$R(t)$	Production rate $\times 10^3$ m^3 per day
S_n	Normalized saturation
S_{or}	Residual oil saturation
S_w	Water saturation
S_{wc}	Connate water saturation
V	Volume (stock tank m^3)
ϕ	Porosity (m^3/m^3)
μ_o	Oil viscosity (cP)
μ_w	Water viscosity(cP)

Table A2. *Abbreviations*

Abbreviation	Meaning
FED	Factorial experimental design
K&B	Kyte & Berry
NMD	Normalized maximum difference
NRMS	Normalized root mean square
PCE	Capillary pressure equilibrium
PVW	Pore volume weighted
RMS	Root mean square
STO	Stone
STOIIP	Stock tank oil initially in place

APPENDIX B: FACTORIAL EXPERIMENTAL DESIGN

A full factorial two-level experimental design consists of varying N parameters through all combinations of high and low values and observing the variable y. Then if the parameter vector follows a linear combination of all parameters and interactions, the coefficients of the equation:

$$y(\underline{x}) = y_{mean} + \sum_{i=1}^{n} a_i x_i + \sum_{i=1}^{n}\sum_{\substack{j=1 \\ j\neq i}}^{n} b_{i,j} x_i x_j + \sum_{i}^{n}\sum_{j=i+1}^{n}\sum_{k=j+1}^{n} c_{i,j,k} x_i x_j x_k + \ldots \quad \text{(B1)}$$

can be obtained where $\underline{x}$ is a binary parameter vector of values+1 and −1 values representing the normalized parameter maximum and minimum, respectively, y_{mean} is the arithmetic average of y over $2N$ runs and the *a*s, *b*s and *c*s represent the measure of the effect (i.e. coefficients) of each variable. These coefficients can be obtained by simultaneous solution or by Yates method (1937; see also Box *et al.* 1978, ch. 10, for details).

Equation (B1) can be rewritten as:

$$y(\underline{x}) = \sum_{i=0}^{2^N-1} \alpha_i \prod_{j=1}^{N} x_j^{p_i} \quad \text{(B2)}$$

where *a*s are the coefficients in equation (B1) and p is a binary representation of j, p_i is the i^{th} digit in p and is 0 or 1. For example for N=10 and i=895, then p='1110000000' and refers to the interaction between parameters x_1, x_2 and x_3. The nomenclature of p in Figures 11 and 12 is used.

The European Commission is thanked for partly funding SAIGUP under the EU Fifth Framework Hydrocarbons Reservoir Programme. Schlumberger Geoquest is thanked for use of the Eclipse simulator and Roxar for use of RMS and MORE. We are grateful to Badley Geoscience, BG International, Roxar and Shell for their support of the SAIGUP project and for their sponsorship of the production of this thematic set.

REFERENCES

Barker, J.W. & Thibeau, S. 1997. A Critical Review of the Use of Pseudorelative Permeabilities for Upscaling. *SPE Reservoir Evaluation,* **12**, 138–143.

Box, G.E.P. & Hunter, J.S. 1961. The 2^{k-p} Fractional Factorial Design. Part I. *Technometrics,* **3**, 311–351.

Box, G.E.P., Hunter, W.G. & Hunter, J.S. 1978. Statistics for Experimenters: An Introduction to Design, Data Analysis, and Model Building. John Wiley and Sons, New York, 291–433.

Christie, M. A., Mansfield, M., King, P. R., Parker, J. W. & Culverwell, I. D. 1995. A Renormalisation-Based Upscaling Technique for WAG floods in Heterogeneous Reservoirs. Paper SPE 29127, presented at the 13th SPE Symposium on Reservoir Simulation, San Antonio, Texas, 12–15 February.

Christie, M.A. 2001. Flow in Porous Media – Scale Up of Multiphase Flow. *Current Opinion in Colloid and Interface Science,* **6**, 236–241.

Coll, C. & Muggeridge, A.H. 2001. Regional Upscaling: A New Method To Upscale Waterflooding in Heterogeneous Reservoirs for a Range of Capillary and Gravity Effects. *SPE Journal,* **66**, 299–310.

Corbett, P.W.M. 1993. *Reservoir Characterisation of a Laminated Sediment. The Rannoch Formation, Middle Jurassic, North Sea.* PhD Thesis. Heriot-Watt University, Edinburgh.

Corbett, P. W. M., Ringrose, J. L. & Sorbie, K. S. 1992. Laminated Clastic Reservoirs: The Interplay of Capillary Pressure and Sedimentary Architecture. Paper SPE 24699, presented at the 68th Annual Technical Conference, Washington DC, 4–7 October.

Damsleth, E., Hage, A. & Volden, R. 1992. Maximum Information at Minimum Cost: A North Sea Field Development Study with an Experimental Design. *Journal of Petroleum Technology,* **December**, 1350–1356 (paper SPE 23139).

Darman, N. H., Sorbie, K. S. & Pickup, G. E. 1999. The Development of Pseudo Functions for Gravity-Dominated Immiscible Gas Displacements. Paper SPE 51941, presented at the SPE Reservoir Simulation Symposium, Houston, Texas, 14–17 February.

Daws, J.A. 1992. *Sedimentology, Diagenesis and Reservoir Characterization of the Brent Group in the North Viking Graben-East Shetland Basin, Northern North Sea.* PhD thesis. University of Aberdeen, UK.

Daws, J.A. & Prosser, D.J. 1992. Scales of Permeability Heterogeneity within the Brent Group. *Journal of Petroleum Geology,* **54**, 397–418.

Dupouy, P., Barker, J.W. & Valois, J-P. 1998. Grouping Pseudo Relative Permeability Curves. *In Situ,* **22**, 1–33.

Eclipse Manual, 2003. Schlumberger Geoquest.

Ekrann, S., Dale, M., Langaas, K. & Mykkeltveit, J. 1996. Capillary Limit Effective Two-Phase Properties for Three-dimensional Media. Paper SPE 35491, presented at the European 3-D Reservoir Modelling Conference, Stavanger, Norway, 16–17 April.

Howell, J.A., Skorstad, A., MacDonald, A., Fordham, A., Flint, S., Fjellvoll, B. & Manzocchi, T. 2008. Sedimentological parameterization of shallow-marine reservoirs. *Petroleum Geoscience,* **14**, 17–34.

Jones, A., Doyle, J., Jacobsen, T. & Kjønsvik, D. 1995. Which sub-seismic heterogeneities influence waterflood performance? A case study of low net to gross fluvial reservoirs. *In:* De Haan, H.J. (ed.) *New Developments in Improved Oil Recovery.* Geological Society, London, Special Publications, **84**, 5–18.

Kortekaas, T.F.M. 1985. Water/Oil Displacement Characteristics in Cross-bedded Reservoir Zones. *SPE Journal,* **25**, 917–926.

Kumar, A. T. & Jerauld, G. R. 1996. Impact of Scale-up on Fluid Flow, from Plug to Gridblock Scale in Reservoir Rock. Paper SPE 35452, presented at the SPE/DOE Tenth Symposium on Improved Oil Recovery, Tulsa, 21–24 April.

Kyte, J.R. & Berry, D.W. 1975. Pseudo Functions to Control Numerical Dispersion. *SPE Journal,* **15**, 269–275.

Manzocchi, T., Carter, J.N. & Skorstad, A. 2008*a*. *et al.* Sensitivity analysis of the impact of geological uncertainty on production from faulted and unfaulted shallow-marine oil reservoirs: objectives and methods. *Petroleum Geoscience,* **14**, 3–15.

Manzocchi, T., Matthews, J.D. & Strand, J.A. 2008*b*. *et al.* A study of the structural controls on oil recovery from shallow-marine reservoirs. *Petroleum Geoscience,* **14**, 55–70.

Matthews, J.D., Carter, J.N., Stephen, K.D., Zimmerman, R.W., Skorstad, A., Manzocchi, T. & Howell, J.A. 2008. Assessing the effect of geological uncertainty on recovery estimates in shallow-marine reservoirs: the application of reservoir engineering to the SAIGUP project. *Petroleum Geoscience,* **14**, 35–44.

Opdal, S. T. & Kossack, C. A. 1990. The Interaction of Small and Medium Scale Heterogeneities from a Shallow Marine Depositional Environment with Various Two-Phase Displacements. Paper SPE 21072, presented at the SPE Latin American Petroleum Engineering Conference, Rio de Janiero, Brazil, 14–19 October.

Peng, C. Y. & Gupta, R. 2003. Experimental Design in Deterministic Modelling: Assessing Significant Uncertainties. Paper SPE 80537, presented at the SPE Asia and Pacific Oil and Gas Conference, Jakarta, Indonesia, 9–11, September.

Pickup, G.E. & Sorbie, K.S. 1996. The Scaleup of Two-phase Flow in Porous Media Using Phase Permeability Tensors. *SPE Journal,* **1**, 369–381.

Pickup, G.E. & Stephen, K.D. 2000. An assessment of steady state scale up methods for small-scale geological models. *Petroleum Geoscience,* **6**, 203–210.

Ringrose, P.S., Sorbie, K.S., Corbett, P.W.M. & Jensen, J.L. 1993. Immiscible Flow Behaviour in Laminated and Cross-bedded Sandstones. *Journal of Petroleum Science and Engineering,* **9**, 103–124.

Skorstad, A., Kolbjørnsen, O., Manzocchi, T., Carter, J.N. & Howell, J. 2008. Combined effects of structural, stratigraphic and well controls on production variability in faulted shallow-marine reservoirs. *Petroleum Geoscience,* **14**, 45–54.

Smith, E.H. 1991. The Influence of Small Scale Heterogeneity on Average Relative Permeability. *In:* Lake, L.W., Carroll, H.B. & Wesson, T.C. (eds) *Reservoir Characterization II.* Academic Press, San Diego, 52–76.

Stephen, K.D., Pickup, G.E. & Sorbie, K.S. 2001. The Local Analysis of Changing Force Balances in Immiscible Incompressible Two-Phase Flow. *Transport in Porous Media,* **45** (1), 63–68.

Stephen, K. D., Pickup, G. E. & Clark, J. 2003. Modelling and Flow Simulations of a North Sea Turbidite Reservoir: Sensitivities and Upscaling. Paper SPE 78292, presented at the 13th European Petroleum Conference, Aberdeen, Scotland, 29–31 October.

Stone, H. L. 1991. Rigorous Black Oil Pseudo Functions. Paper SPE 21207, presented at the SPE Symposium on Reservoir Simulation, Anaheim, California, 17–20 February.

Weber, K.J. 1986. How Heterogeneity Affects Oil Recovery. *In:* Lake, L.W. & Carroll, H.B. (eds) *Reservoir Characterization.* Academic Press, Florida.

Whitaker, S. 1969. Advances in the Theory of Fluid Motion in Porous Media. *Industrial Chemistry,* **12**, 14–28.

White, C. D. & Royer, S.A. 2003. Experimental Design as a Framework for Reservoir Studies. Paper SPE 79676, presented at the SPE Reservoir Simulation Symposium, Huston, Texas, USA, 3–5 February.

White, C. D., Willis, B. J., Narayanan, K. & Dutton, S. P. 2000. Identifying Controls on Reservoir Behaviour Using Designed Simulations. Paper SPE 62971, presented at the SPE Annual Technical Conference and Exhibition, Dallas, Texas, USA, 1–4 October.

Yang, C. & Stephen, K.D. 2002. Investigation of the Effects of Small-Scale Uncertainty on Upscaling Using Factorial Experimental Design, Work Package 3.1 Upscaling Update. Annex 3 of the 24 month report of the SAIGUP project, EU62002ENK6CT-2000-00073.

Yang, C., Stephen, K.D., Ma, J. & Pickup, G.E. 2004. Investigation of the Effects of Small-Scale Uncertainty on Upscaling Using Factorial Experimental Design. Annex 10 of the Final report of the SAIGUP project, EU62004ENK6CT-2000-00073.

Yates, F. 1937. *The Design and Analysis of Factorial Experiments.* Imperial Bureau of Soil Science, Bulletin, **35**.

Received 29 January 2007; revised typescript accepted 15 October 2007.